

Identification of human brain regions underlying responses to resistive inspiratory loading with functional magnetic resonance imaging

DAVID GOZAL^{†‡§}, OMID OMIDVAR[†], KONRAD A. T. KIRLEW[¶], GASSER M. HATHOUT[¶], REX HAMILTON[¶], ROBERT B. LUFKIN[¶], AND RONALD M. HARPER[†]

Departments of [†]Anatomy and Cell Biology and [¶]Radiology, University of California School of Medicine, Los Angeles, CA 90095; and [‡]Division of Neonatology and Pediatric Pulmonology, Childrens Hospital, University of Southern California School of Medicine, Los Angeles, CA 90027

Communicated by Charles H. Sawyer, University of California School of Medicine, Los Angeles, CA, April 6, 1995 (received for review February 9, 1995)

ABSTRACT Compensatory ventilatory responses to increased inspiratory loading are essential for adequate breathing regulation in a number of pulmonary diseases; however, the human brain sites mediating such responses are unknown. Midsagittal and axial images were acquired in 11 healthy volunteers during unloaded and loaded (30 cmH₂O; 1 cmH₂O = 98 Pa) inspiratory breathing, by using functional magnetic resonance imaging (fMRI) strategies (1.5-tesla MR; repetition time, 72 msec; echo time, 45 msec; flip angle, 30°; field of view, 26 cm; slice thickness, 5 mm; number of excitations, 1; matrix, 128 × 256). Digital image subtractions and region of interest analyses revealed significantly increased fMRI signal intensity in discrete areas of the ventral and dorsal pons, interpeduncular nucleus, basal forebrain, putamen, and cerebellar regions. Upon load withdrawal, certain regions displayed a rapid fMRI signal off-transient, while in others, a slower fMRI signal decay emerged. Sustained loading elicited slow decreases in fMRI signal across activated regions, while second application of an identical load resulted in smaller signal increases compared to initial signal responses ($P < 0.001$). A moderate inspiratory load is associated with consistent regional activation of discrete brain locations; certain of these regions have been implicated in mediation of loaded breathing in animal models. We speculate that temporal changes in fMRI signal may indicate respiratory after-discharge and/or habituation phenomena.

Adequate perception and response to added inspiratory loads is an essential component for ventilatory regulation in a number of pulmonary diseases. Diminished perception to respiratory loads (1) or reduced voluntary activation of the diaphragm (2) have been recently documented in asthmatic patients and appear to play a significant role in abrupt onset of respiratory failure or sudden death in asthma (3). Reversibly diminished ventilatory compensation to added inspiratory loads also occurs in patients with moderate to severe obstructive sleep apnea syndrome during wakefulness (4), indicating that inappropriate respiratory load responses are common across multiple lung diseases.

External application of mild to moderate inspiratory resistive loads results in prolongation of inspiratory time and inspiratory drive and reduces breathing frequency but results in almost no change from baseline minute ventilation (5–7). The findings suggest exquisite regulation of breathing for metabolic needs in normal subjects undergoing short-duration loads by close integration of neural systems mediating inspiratory and expiratory timing. Coordination of such timing depends heavily on the integrity of pontine regions (8), which receive substantial mechanoreceptor input from vagal affer-

ents. Animal evidence suggests that, in addition to pontine regions, cerebral, forebrain, midbrain, and cerebellar structures exert facilitatory influences on respiratory pattern generation underlying responses to ventilatory loads (9–11). Central respiratory control regions must also integrate diverse afferent inputs from other sensors, including chemoreceptors, to generate ventilatory output sufficient to maintain a narrow homeostatic range for blood gases.

However, the location of brain structures mediating ventilatory responses to inspiratory loads in humans remains speculative and can only be inferred from correlations between defined brain lesions and specific ventilatory disturbances (12, 13). Determination of such locations and the time course of responses within these sites would provide important theoretical insights into normal ventilatory control mechanisms and assist in determination of mechanisms that mediate disrupted control in pulmonary disease.

Functional magnetic resonance imaging (fMRI) techniques provide a noninvasive procedure to visualize human brain sites activated to specific stimuli or tasks (14–17). Such procedures showed that regional neural activation follows central chemoreceptor excitation induced by changes in inspired CO₂ concentrations (18). Furthermore, hypercapnia induced widespread distribution of activated sites, suggesting that multiple brain structures underlie the overall response to increased CO₂. By using fMRI strategies, we aimed to localize brain regions participating in the response to added inspiratory loads in healthy human subjects. Portions of this work have been presented (19).

METHODS

Subjects. Eleven healthy volunteers (nine males and two females), aged 27–48 years, were studied, after giving informed consent. The study was approved by the Institutional Review Board at UCLA.

MRI. Imaging was performed with a 1.5-tesla MR scanner (General Electric Signa System, Milwaukee, WI), using a standard head coil, at the UCLA Center for the Health Sciences. To minimize subject and head movement during the scanning procedure, appropriate attachments with snug-fitting foam were used. Routine T1-weighted coronal and sagittal scout images were performed to identify the planes for subsequent imaging.

Spoiled gradient acquisition in a steady-state imaging was performed by using the following parameters: repetition time, 72 msec; echo time, 45 msec; flip angle, 30°; 128 × 256 matrix;

Abbreviations: MR, magnetic resonance; MRI, MR imaging; fMRI, functional MRI; ROI, region of interest.

[§]To whom reprint requests should be sent at the present address: Section of Pediatric Pulmonology, SL-37, University of Tulane School of Medicine, 1430 Tulane Avenue, New Orleans, LA 70112.

The publication costs of this article were defrayed in part by page charge payment. This article must therefore be hereby marked "advertisement" in accordance with 18 U.S.C. §1734 solely to indicate this fact.

number of excitations, 1; field of view, 26 cm with a 5-mm slice thickness. Images were acquired from three different planes during baseline and inspiratory loading conditions: one sagittal plane slightly off midline (Fig. 1A), and two axial planes—across the pons (Fig. 1C, plane a) and across the cerebral peduncles (Fig. 1C, plane b). Each scan required ≈ 9.5 sec.

Stability of the MR unit was verified with serial spoiled gradient acquisition in a steady-state imaging of a standard Daily Quality Assurance phantom (model 46-28297861; GE Medical Systems). Sixty images were intermittently obtained over an 18-min period, and no signal drift was observed. The average signal variation ranged from 0.18 to 0.34% in high and low signal intensity regions of the phantom, respectively.

Test Protocol. Subjects were imaged while lying comfortably in the scanner and breathing via a mouthpiece through a two-way nonrebreather respiratory valve (Hans Rudolph, Kansas City, MO) with nose clips. The dead space of the system was ≈ 40 ml, and resistance to airflow was determined at <0.012 cmH₂O per liter per min for flow rates ranging from 0 to 200 liters/min (1 cmH₂O = 98 Pa). Fifteen images were acquired during baseline unloaded conditions. Subjects then breathed through a flow-resistive load or resistor applied to the inspiratory limb of the nonrebreather valve, which consisted of a plastic tube 4 mm in diameter and 100 mm in length, eliciting an approximately constant resistance of 30 cmH₂O per liter per sec at flows between 5 and 30 liters/min. A second set of 15

images was obtained, after which the load was removed, and 60 additional images were consecutively acquired. At this point, the load was reapplied, and 45 images were successively obtained.

Ventilatory Measurements. In four subjects, ventilatory measurements during unloaded and loaded conditions were performed while the subject was in the supine position and breathing through the same respiratory apparatus used for scanning procedures. PO₂ and PCO₂ were sampled continuously at the expiratory port of the breathing valve and analyzed by using a mass spectrometer on a breath-by-breath basis (Perkin-Elmer 1100 medical gas analyzer; Applied Science Division, Pomona, CA). Flow was measured by using a heated pneumotach and a pressure transducer (Valydine, Northridge, CA). Breath-by-breath tidal volume was obtained by analog integration of the flow signal. All outputs were recorded on a Gould polygraph strip chart recorder (Gould, Rolling Meadows, IL).

Inspiratory time, total time, tidal volume, and end-expiratory CO₂ tension were measured for each breath, and from these assessments, respiratory rate and minute ventilation were calculated.

Data Analysis. Images from each subject were transferred to a Sun Sparc Station 2 (Sun Microsystems, Mountain View, CA). Each image collected under the experimental condition was digitally subtracted from the average image obtained during baseline by using an image processing routine written in

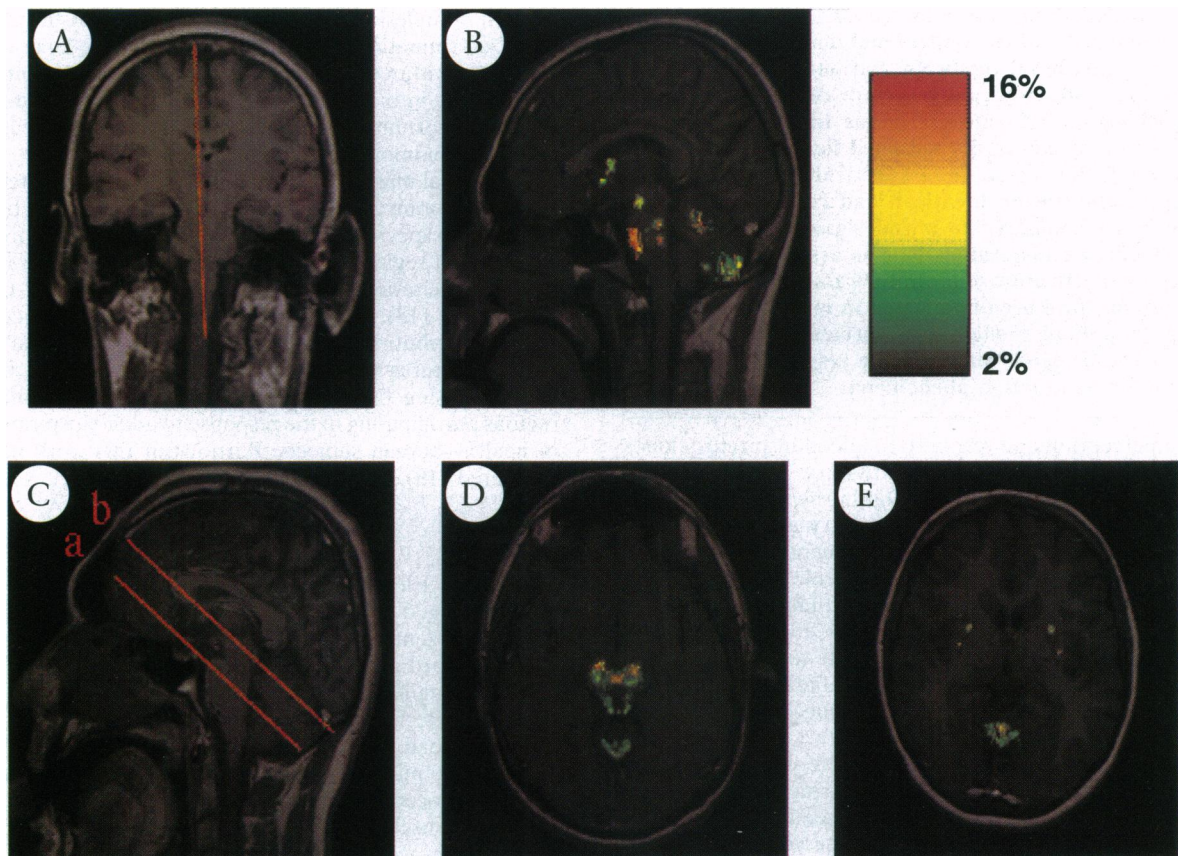


FIG. 1. (A) Coronal T1 section in one subject. Red line indicates the fMRI sagittal imaging plane. (B) Midsagittal T1 image in one subject. Regions revealing significant fMRI signal enhancements during application of an inspiratory resistive load in all 11 subjects are shown on a pseudocolored scale in which each pixel was assigned either a transparent value, when fMRI signal change did not achieve statistical significance, or a pseudocolored scale rank corresponding to a statistically significant percent signal increase. The pseudocolored scale colors range from green (fMRI signal increase of 2%) to red (maximal fMRI signal increase of 16% as indicated). (C) Sagittal T1 image in another subject to illustrate the slice locations chosen for axial fMRI acquisitions. Red line a indicates a midpontine cut and red line b indicates midcerebral peduncle cut. (D) Axial T1 image across the midpons in one subject. Regions revealing significant fMRI signal enhancements during application of an inspiratory resistive load in 11 subjects are shown on a pseudocolored scale as described above. (E) Axial T1 image at the midcerebral peduncular plane in one subject. Regions revealing significant fMRI signal enhancements during application of an inspiratory resistive load in 11 subjects are shown on a pseudocolored scale as described above.

ANSI C. The resultant subtraction images were then averaged and subjected to ANOVA procedures on a pixel-by-pixel basis. In addition, resultant gray-scale subtraction displays were pseudo-colored with reference to a difference scale that corresponded to a *P* value of <0.01. Region of interest (ROI) analysis for signal intensity was performed for each image in regions determined from visual inspection of activation images. Defined ROI, ranging from 6 to 64 mm² (6–64 pixels), were placed in every activated region, while avoiding visible vessels, inner table of skull, or cerebrospinal fluid-containing areas. Average pixel intensities from each ROI were obtained on all images from each subject to generate signal intensity vs. time curves.

For each subject, percentage frame-by-frame changes from baseline were calculated for each ROI by subtraction from the average ROI value of the initial 15 frames. In addition, ROI percent change was averaged across subjects for each image, and ROI locations across different subjects were matched from individual anatomical landmarks for graphic purposes.

Values for baseline and initial and subsequent inspiratory loaded conditions were then subjected to ANOVA procedures followed by post hoc tests using BMDP statistical software (University of California, Berkeley). A *P* value of <0.05 was required to reach statistical significance.

RESULTS

Activated Regions. Significant increases in fMRI signal intensity occurred during inspiratory loads in several discrete brain locations (Fig. 1). In the sagittal plane, two regions of the dorsal pons, corresponding to the parabrachial region at the level of the Vth motor nucleus and the locus coeruleus, displayed activation patterns. More ventrally, increased activity developed in the basis pontis and, rostrally within the midbrain, in the interpeduncular nucleus in the area of Tsai. The basal forebrain and putamen and areas within the cerebellum (culmen and central vermis) displayed significant signal increases (Fig. 1B). In the more caudally placed axial plane, significant MR signal increases occurred in pontine and cerebellar regions (Fig. 1D). Signal enhancements in regions within the putamen of lentiform nucleus, close to globus pallidus, were observed bilaterally and portions of tuber and uvula cerebellar regions (Fig. 1E).

Signal Dynamics. Mean peak changes in the different regions during initial stimulus application and mean peak changes occurring during second load application are shown in Table 1. In general, a significant decrease in the magnitude of MR signal change was observed at all ROI sites in which a significant signal response occurred with the second load.

Frame-by-frame signal analysis during initial load application revealed two different MR signal off-transient patterns (Fig. 2). In some locations, such as the basal pons, putamen, and uvula of the cerebellum, an immediate signal return to baseline occurred upon discontinuation of the resistor (Fig. 2B). In contrast, both dorsal and ventral pontine structures, cerebellar vermis, and basal forebrain regions displayed a slow signal decrease to baseline values, despite inspiratory load removal (Figs. 2A and 3).

Sustained application of the inspiratory resistor resulted in progressive MR signal decreases over time at all activation sites to values similar to those measured during baseline conditions (Fig. 4). The onset of significant signal decreases occurred after ≈3 min of constant added inspiratory resistance (range, 150–225 sec). Both onset and signal decrease rate over time were similar for all activated sites.

Two subjects underwent a second identical study on a different occasion (within 30 and 45 days, respectively), and virtually identical signal increases and activated locations emerged in both studies.

Ventilatory Measures. In all four subjects who underwent ventilatory measurements, increases in inspiratory time ($27.4 \pm 7.5\%$) and tidal volume ($22.4 \pm 4.5\%$) and decreases in

Table 1. Peak changes in MR signal intensity in various regions of interest upon application of an inspiratory load

Site	% change		<i>P</i> value
	I	II	
Ventral pons			
Sagittal	16.31 ± 2.7	9.72 ± 1.77	<0.001
Axial	14.4 ± 1.61	9.26 ± 3.08	<0.001
Dorsal pons			
Sagittal	14.08 ± 2.50	5.57 ± 1.21	<0.001
Axial	12.10 ± 2.73	8.46 ± 2.92	<0.01
Cerebral peduncle (sagittal)	11.15 ± 1.45	8.71 ± 1.01	<0.005
Rostral cerebellum			
Sagittal	9.59 ± 0.97	5.48 ± 0.77	<0.001
Axial	8.6 ± 0.79	6.29 ± 1.12	<0.01
Caudal cerebellum (sagittal)	6.94 ± 1.55	4.53 ± 0.83	<0.02
Thalamus (sagittal)	7.95 ± 1.39	5.73 ± 1.33	<0.02
Hypothalamus (sagittal)	9.97 ± 1.26	6.25 ± 0.26	<0.001
Putamen (axial)			
Left	8.51 ± 1.65	7.38 ± 0.36	<0.05
Right	8.46 ± 1.58	7.32 ± 0.35	<0.05
Caudate nucleus			
Left	10.36 ± 0.71	6.92 ± 1.46	<0.001
Right	9.92 ± 0.79	6.67 ± 1.38	<0.001

I and II, first and second application of inspiratory load. Data are the mean ± SEM.

respiratory rate ($12.6 \pm 3.6\%$) with no significant minute ventilation changes occurred immediately (first breath) upon application of the resistor. In addition, mild end-expiratory CO₂ tension decreases developed during loaded breathing (from 42.4 ± 0.8 torr to 36.7 ± 1.4 torr; *P* < 0.05; 1 torr = 133.3 Pa). Discontinuation of the inspiratory load was not associated with immediate return of ventilatory measures to pre-load conditions but rather with a slow tidal volume reduction over time (20–30 sec), unchanged respiratory rate, and relative alveolar hyperventilation such that further small end-expiratory CO₂ tension decreases occurred.

DISCUSSION

Discrete regions of neural activation emerged in response to added inspiratory loads in humans. Activation of these regions

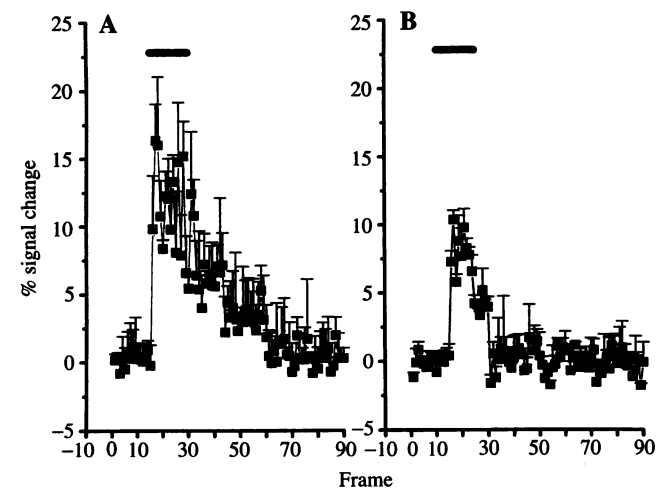


Fig. 2. Frame-by-frame fMRI signal changes in regions of interest located in parabrachial pons (A) and putamen (B) during short-duration (≈150 sec) inspiratory resistive loading (mean ± SD). Thick horizontal lines indicate resistive inspiratory load stimulus.

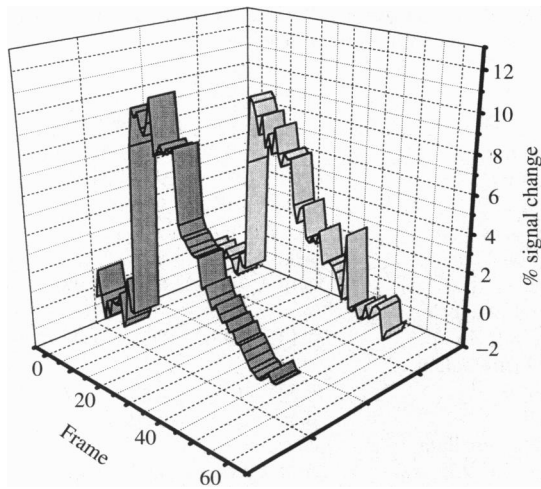


FIG. 3. Individual frame-by-frame fMRI signal tracings of a region of interest located in basal forebrain in two subjects. The inspiratory resistive load was applied after 15 initial baseline frames and was removed immediately upon further acquisition of 15 images. Note slow fMRI signal return to baseline values after stimulus discontinuation.

was reproducible, and particular regions demonstrated divergent signal kinetics upon discontinuation of the inspiratory load. Subsequent application of the inspiratory resistor resulted in a reduced magnitude of MR signal response increases, while sustained inspiratory loads led to progressive return of MR signal to baseline values despite ongoing stimulation.

Neural activation is associated with complex regional alterations in focal blood flow (20), cerebral blood volume and oxygen extraction (21), and cellular metabolism and oxygen utilization (22–24). One initial consequence of this elaborate interplay is a net increase in regional oxyhemoglobin/deoxyhemoglobin ratios (14, 25) that has been confirmed by using near-infrared spectroscopy (26) and can be readily identified as signal increases by gradient echo and T2*-weighted echo-planar MRI.

The vast majority of earlier studies on neuronal activation employed either high-strength magnetic field scanners or echo-planar imaging. However, use of a widely available standard 1.5-T MRI system provides useful data during sensorimotor activation tasks (27). The magnitude of MR signal

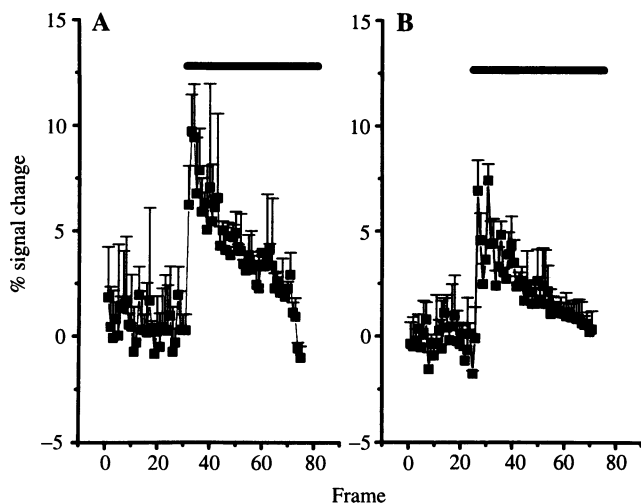


FIG. 4. Frame-by-frame fMRI signal changes in regions of interest located in parabrachial pons (*A*) and putamen (*B*) during prolonged (≈ 450 sec) inspiratory resistive loading (mean + SD). Thick horizontal lines indicate resistive inspiratory load stimulus.

intensity changes observed in this study is similar to that found during motor task activation, such that signal changes as large as 20% can be obtained by improved signal-to-noise ratio routines (28, 29). The inherent variability of functional MRI signal is dependent on the magnetic field strength (30) and may also be affected by white matter density of the imaged structure (31). In addition, involuntary motion artifacts or proximity to bone cavities and large blood vessels may induce magnetic field inhomogeneities and pulsatile artifacts. However, brain regions such as spinal cord and lateral geniculate nucleus have been imaged during specific sensorimotor tasks (32, 33). Furthermore, a simple motor task such as finger tapping elicits fMRI signal changes on the order of 7–10 standard deviations above the intrinsic variability of the signal when the subject is at rest, and current results concur with these findings (34). Therefore, although particular care is mandatory in interpretation of the topographic extent of regional activation, locations demonstrating significant fMRI signal changes in this study should be viewed as the most likely neural population candidates underlying the response to inspiratory resistive loads.

Certain locations that increased regional activity during inspiratory loads coincide with previously recognized sites underlying the ventilatory response to resistive loads in animals. The parabrachial pons receives significant afferent inputs via vagal and spinal sources from the lungs and chest wall stretch receptors, which are activated by the inspiratory loading task (35). Such thoracic contributions may account for the observed MRI signal increases in dorsal pontine structures. The basal pontine nuclei mediate significant contributions to the cerebellum. The cerebellum has been implicated in classic literature (36) as an important modulator of respiratory-cardiovascular reflexes and in more recent studies (10) as contributing to resistive loading responses. The locus coeruleus plays a significant role in recruiting adrenergic fibers for arousal, demonstrates primary vagal afferent depolarization (37), and may mediate important aspects of concomitant blood pressure alterations to increased respiratory efforts with loaded breathing. Although we did not examine cortical regions in this study, the cerebrum has also been implicated in loaded (9) and voluntary respiratory maneuvers (38). Interactions between the rostral structures and interpeduncular nuclei may underlie the higher cortical influences demonstrated in animals. Contributions from the basal ganglia and midline ventral and dorsal pontine activation appear to be bilateral.

The dynamics of MR signal decay after discontinuation of the inspiratory load suggest differential response patterns at regional sites to mediation of loaded breathing. Certain sites exhibited immediate signal return to baseline values, while in other regions, the MR signal progressively decreased over time. Ventilatory measurements in all four subjects confirmed that discontinuation of the resistive load was associated with a gradual rather than immediate return of ventilatory components to baseline. Application of resistive inspiratory loads may elicit short-term potentiation or system inertia mechanisms that translate into slowly diminishing ventilation upon load removal (39). We postulate that regions in which slow MR signal decrements occurred may underlie the source of short-term memory respiratory mechanisms in humans.

The physiological mechanisms that mediate reduced MR signal changes during subsequent load application are unclear. One explanation is that rapid habituation occurs (40), thereby leading to decreased ventilatory response with parallel decrease in neural recruitment. Alternatively, neural "learning" may occur, whereby the initial load requires an increased number of neurons to achieve the desired ventilatory response, while subsequent challenges will elicit lesser neuronal recruitment to achieve similar ventilatory effects in a fashion comparable to other motor learning tasks (41).

Sustained inspiratory loads lead to a biphasic dynamic MR signal decrease over time, characterized by immediate signal increases during the initial stimulation phase, followed by signal decreases to near baseline or even subbaseline values despite continuing challenge. These temporal characteristics are similar to those previously found in the calcarine cortex during sustained photic stimulation (42) and suggest that stimulus duration is an important determinant of MR signal response. The current concept of increased MR T2* signal as indicative of neural activity assigns discrepant changes in regional blood flow and oxygen utilization during early phases of neuronal discharge (14). As a result of "excessive" arterial blood flow to the activated site and the concomitant preferentially glycolytic nonoxidative metabolism of firing neurons (23), intracellular lactate increases and a substantial decrease in deoxyhemoglobin concentration occurs in the venous capillary phase. Such a decrease in deoxyhemoglobin diminishes intravoxel dephasing and increases signal intensity when T2*-weighted sequences are employed. However, with prolonged stimulation, it is unlikely that continued anaerobic cellular metabolism will persist. Instead, aerobic energy utilization would be expected to take over, leading to tight coupling of regional blood flow and oxygen needs and to decreasing intracellular lactate in activated neurons (43). Such a transition would be accompanied by a gradual return of venous deoxyhemoglobin concentrations to either baseline or above baseline levels and, consequently, would induce reciprocal changes in T2* MR signal intensity. The temporal characteristics of the transition from a primarily anaerobic to a predominantly aerobic process of neuronal discharge may be both individually determined and unique to the type and function of neuronal populations intervening in the response to the stimulus. For example, during constant photic stimulation, significant MR signal decreases developed between 2 and 5 min (42). Stimulus type, paradigm duration, and timing of signal acquisition are all critically dependent on the window of opportunity offered by T2* MR signal kinetics.

In conclusion, we demonstrate increased activity in specific brain locations during mild resistive inspiratory loading in awake humans. Regional differences in MRI signal time course during application of the respiratory load and after removal of such loads demonstrate differential signal kinetics that may underlie neural phenomena playing an important role in adaptation in lung health and disease states.

This study was supported by National Institutes of Health Grants HD-22506 and HL-22418. D.G. is the recipient of a Parker B. Francis Fellowship in Pulmonary Research. This work served in partial fulfillment of the requirements for an M.D. thesis from the Faculté de Médecine de Rouen, France (O.O.).

- Kiruchi, Y., Okabe, S., Tamura, G., Hida, W., Homma, M., Shirato, K. & Takishima, T. (1994) *N. Engl. J. Med.* **330**, 1329-1334.
- Allen, G. M., McKenzie, D. K., Gandevia, S. C. & Bass, S. (1993) *Respir. Physiol.* **93**, 29-40.
- Allen, G. M., Hickie, I., Gandevia, S. C. & McKenzie, D. K. (1994) *Thorax* **49**, 881-884.
- Greenberg, H. E. & Scharf, S. M. (1993) *Am. Rev. Respir. Dis.* **148**, 1610-1615.
- Altose, M. D., Kelsen, S. G. & Chemiack, N. S. (1979) *Respir. Physiol.* **36**, 249-260.
- Axen, K. & Haas, S. S. (1979) *J. Appl. Physiol.* **46**, 743-751.
- Daubenspeck, J. A. & Bennett, F. M. (1983) *J. Appl. Physiol.* **55**, 1160-1166.
- Cohen, M. I. & Feldman, J. L. (1984) *J. Neurophysiol.* **51**, 753-776.
- Xu, F., Taylor, R. F., McLarney, T., Lee, L. & Frazier, D. T. (1993) *J. Appl. Physiol.* **74**, 853-858.
- Xu, F., Taylor, R. F., Lee, L. & Frazier, D. T. (1993) *J. Appl. Physiol.* **75**, 675-681.
- Hugelin, A. (1986) in *Handbook of Physiology: The Respiratory System; Control of Breathing*, eds. Fishman, A. P., Cherniack, N. S. & Widdicombe, J. G. (Am. Physiol. Soc., Bethesda), pp. 69-91.
- Kinney, H. C., Filiano, J. J., Brazy, J. E., Burger, P. C. & Sidman, R. L. (1989) *Clin. Neuropathol.* **8**, 163-173.
- Beal, M. F., Richardson, E. P., Jr., Brandstetter, R., Hedley-Whyte, E. T. & Hochberg, F. H. (1983) *Neurology* **33**, 717-721.
- Ogawa, S., Tank, D.-W., Menon, R., Ellerman, J.-M., Kim, S.-G., Merkle, H. & Ugurbil, K. (1992) *Proc. Natl. Acad. Sci. USA* **89**, 5951-5955.
- McCarthy, G., Blamire, A. M., Rothman, D. L., Gruetter, R. & Shulman, R. G. (1993) *Proc. Natl. Acad. Sci. USA* **90**, 4952-4956.
- Kwong, K. K., Belliveau, J. W., Chesler, D. A., Goldberg, I. E., Weisskoff, R. M., Poncelet, B. P., Kennedy, B. N., Hoppel, B. E., Cohen, M. S., Turner, R., Cheng, H. M., Brady, T. J. & Rosen, B. R. (1992) *Proc. Natl. Acad. Sci. USA* **89**, 5675-5679.
- Frahm, J., Bruhn, H., Merboldt, K. D. & Hanicke, W. (1992) *J. Magn. Reson. Imaging* **2**, 501-505.
- Gozal, D., Hathout, G. M., Kirlew, K. A. T., Tang, H., Woo, M. S., Zhang, J., Lufkin, R. B. & Harper, R. M. (1994) *J. Appl. Physiol.* **76**, 2076-2083.
- Gozal, D., Omidvar, O., Kirlew, K. A. T., Hathout, G. M., Hamilton, R., Lufkin, R. B. & Harper, R. M. (1994) *Soc. Neurosci. Abstr.* **20**, 563.6.
- Fox, P. T., Mintun, M. A., Raichle, M. E., Miezin, F. M., Allman, J. M. & Van Essen, D. C. (1986) *Nature (London)* **323**, 806-809.
- Fox, P. T. & Raichle, M. E. (1986) *Proc. Natl. Acad. Sci. USA* **83**, 1140-1144.
- Phelps, M. E., Kuhl, D. E. & Mazziotta, J. C. (1981) *Science* **211**, 1445-1448.
- Fox, P. T., Raichle, M. E., Mintun, M. A. & Dence, C. (1988) *Science* **241**, 462-464.
- Prichard, J., Rothman, D., Novotny, E., Petroff, O., Kuwabara, T., Avison, M., Howseman, A., Hanstock, C. & Shulman, R. (1991) *Proc. Natl. Acad. Sci. USA* **88**, 5829-5831.
- Ogawa, S., Lee, T. M., Nayak, A. S. & Glynn, P. (1990) *Magn. Reson. Med.* **14**, 68-78.
- Hoshi, Y. & Tamura, M. (1993) *J. Appl. Physiol.* **75**, 1842-1846.
- Connelly, A., Jackson, G. D., Frackowiak, R. S., Belliveau, J. W., Vargha-Khadem, F. & Gadian, D. G. (1993) *Radiology* **188**, 125-130.
- Schad, L. R., Trost, U., Knopp, M. V., Muller, N. & Lorenz, W. J. (1993) *Magn. Reson. Imaging* **11**, 461-464.
- Fried, I., Gozal, D., Kirlew, K. A. T., Hathout, G. M., Tang, H., Zhang, J. X. & Harper, R. M. (1994) *NeuroReport* **5**, 1593-1596.
- Bandettini, P. A., Wong, E. C., Jesmanowicz, A., Prost, R., Cox, R. W., Hinks, R. S. & Hyde, J. S. (1994) *Proc. Soc. Magn. Reson.* **1**, 434 (abstr.).
- Turner, R., Le Bihan, D., Moonen, C. T. W., Despres, D. & Frank, J. (1991) *Magn. Reson. Med.* **22**, 159-166.
- Yoshizawa, T., Sanders, J. A., Moore, G. J., McKay, M. D., Nose, T. & Sillerud, L. O. (1993) *Proc. Soc. Magn. Reson.* **1**, 55 (abstr.).
- Frahm, J., Merboldt, K. D., Hanicke, W., Kleinschmidt, A. & Steinmetz, H. (1993) *Proc. Soc. Magn. Reson.* **1**, 57 (abstr.).
- DeYoe, E. A., Bandettini, P., Neitz, J., Miller, D. & Winans, P. (1994) *J. Neurosci. Methods* **54**, 171-187.
- Younes, M., Baker, J. & Remmers, J. E. (1987) *J. Appl. Physiol.* **62**, 1502-1512.
- Moruzzi, G. (1940) *J. Neurophysiol.* **3**, 20-32.
- Lucier, G. E. & Sessle, B. J. (1981) *Neurosci. Lett.* **26**, 221-226.
- Ramsey, S. C., Adams, L., Murphy, K., Corfield, D. R., Grootonk, S., Bailey, D. L., Frackowiak, R. S. J. & Guz, A. (1993) *J. Physiol. (London)* **461**, 85-101.
- Leevers, A. M., Simon, P. M., Xi, L. & Dempsey, J. A. (1993) *J. Physiol. (London)* **472**, 749-768.
- Fewell, J. E., Williams, B. J., Szabo, J. S. & Taylor, B. J. (1988) *Pediatr. Res.* **25**, 473-477.
- Jenkins, I. H., Brooks, D. J., Nixon, P. D., Frackowiak, R. S. & Passingham, R. E. (1994) *J. Neurosci.* **14**, 3775-3790.
- Hathout, G. M., Kirlew, K. A. T., So, G. J. K., Hamilton, D. R., Zhang, J. X., Sinha, U., Sinha, S., Sayre, J., Gozal, D., Harper, R. M. & Lufkin, R. B. (1994) *J. Magn. Reson. Imaging* **4**, 537-543.
- Sappey-Mariniere, D., Calabrese, G., Fein, G., Hugg, J. W., Biggins, C. & Weiner, M. W. (1992) *J. Cereb. Blood Flow Metab.* **12**, 584-592.